

## Seismic response of spring-damper-rolling systems with concave friction distribution

Biao Wei<sup>\*1,2</sup>, Peng Wang<sup>1,2a</sup>, Xuhui He<sup>1,2b</sup> and Lizhong Jiang<sup>1,2c</sup>

<sup>1</sup>School of Civil Engineering, Central South University, 22 Shaoshan South Road, Changsha, China

<sup>2</sup>National Engineering Laboratory for High Speed Railway Construction,  
22 Shaoshan South Road, Changsha, China

(Received March 31, 2016, Revised May 24, 2016, Accepted May 27, 2016)

**Abstract.** The uneven distribution of rolling friction coefficient may lead to great uncertainty in the structural seismic isolation performance. This paper attempts to improve the isolation performance of a spring-damper-rolling isolation system by artificially making the uneven friction distribution to be concave. The rolling friction coefficient gradually increases when the isolator rolls away from the original position during an earthquake. After the spring-damper-rolling isolation system under different ground motions was calculated by a numerical analysis method, the system obtained more regular results than that of random uneven friction distributions. Results shows that the concave friction distribution can not only dissipate the earthquake energy, but also change the structural natural period. These functions improve the seismic isolation efficiency of the spring-damper-rolling isolation system in comparison with the random uneven distribution of rolling friction coefficient, and always lead to a relatively acceptable isolation state even if the actual earthquake significantly differs from the design earthquake.

**Keywords:** structure; isolation; concave friction distribution; spring; damper; seismic performance

---

### 1. Introduction

There are limitations for the traditional isolation devices (Ismail *et al.* 2015, Siringoringo and Fujino 2015). With the aim to achieve optimum seismic isolation performance, many researchers have investigated a new kind of rolling-based isolation method (2014 and 2015). Harvey and Gavin (2014) carried out a mathematical model and experimental validation for double rolling isolation systems (RISs), and the effects of the initial conditions, the mass of the isolated object, and the amplitude and period of the disturbance on the system's performance were assessed. Simultaneously, Harvey, Zehil and Gavin (2014) presented a simplified model that was applicable to RISs with any potential energy function. The model was validated through the successful prediction of peak responses for a wide range of disturbance frequencies and intensities. Harvey

---

\*Corresponding author, Associate Professor, E-mail: [weibiao@csu.edu.cn](mailto:weibiao@csu.edu.cn)

<sup>a</sup>Graduate Research Assistant, E-mail: [wangpeng192318@csu.edu.cn](mailto:wangpeng192318@csu.edu.cn)

<sup>b</sup>Professor, E-mail: [xuhuihe@csu.edu.cn](mailto:xuhuihe@csu.edu.cn)

<sup>c</sup>Professor, E-mail: [lzhjiang@csu.edu.cn](mailto:lzhjiang@csu.edu.cn)

and Gavin (2015) proposed a novel reduced order modeling approach to examine the performances of lightly- and heavily-damped RISs located within earthquake-excited structures. Ismail and Casas (Ismail *et al.* 2014, Ismail and Casas 2014) investigated a roll-n-cage (RNC) isolator, and validated that RNC was a convenient isolation system in protecting cable-stayed bridges against the near-fault (NF) earthquakes. Ismail (2015) validated that the RNC isolator could be an efficient solution for a seismic design in near-fault zones considering limited seismic gaps. Wang *et al.* (2014) studied the sloped multi-roller isolation devices for seismic protection of equipment and facilities, and obtained an excellent in-plane seismic isolation performance. Chung *et al.* (2015) considered that an isolation system is not very effective when an inappropriate level of damping is used, and proposed a theoretical method which can be used to determine the optimal frictional coefficient of an isolation system. Ortiz, Magluta and Roitman (2015) presented the validation of a numerical model developed for dynamic analysis of buildings with roller seismic isolation bearings by comparing with the experimental results. Jangid and Londhe (1998) developed a theoretical formulation to obtain seismic responses of a multistory building supported by elliptical rolling rods in 1998, which were quite effective in reducing the seismic response of the system without undergoing large base displacements. Jangid (2000) investigated the stochastic response to the earthquake motion of flexible multi-storey shear type buildings isolated by rolling rods with a re-centering device, indicating that the rolling rods were quite effective in reducing the stochastic response of the structure against the earthquake excitation. Antonyuk and Plakhtienko (2004) analyzed the possible states of a system of interacting solids with rolling friction and unilateral sliding friction bonds, and considered that the system can be used for seismic isolation of buildings. By using the rolling mechanisms, a self-centering capability, and some unique friction devices for supplemental energy dissipation, Lee (Ou *et al.* 2010, Lee *et al.* 2010) firstly proposed a roller seismic isolation bearing for use in highway bridges. After investigating seismic behaviors of the proposed bearing through parametric studies, Lee suspected there was something wrong with the calculation method in AASHTO Specifications and suggested further investigations. Harvey and Gavin (2013) presented the modeling of a rolling isolation platform built from four pairs of recessed steel bowls, which could be used to protect objects from the hazards of horizontal shaking. The numerical results showed that uni-axial models could not be used to predict responses of these systems. Simultaneously, Harvey, Wiebe and Gavin (2013) analyzed the chaotic response of a similar rolling-pendulum vibration isolation system. Rich chaotic behavior was exhibited in the case where the response included impacts. As to isolate an entire raised floor in a building, Cui (2012) performed a series of experiments on a concrete ball-in-cone isolator with solid rubber and polyurethane balls, and identified the practicability of the isolation system. Similarly, Luís Guerreiro (2007) carried out a seismic test and a numerical modeling of a rolling-ball isolation system to protect some light structures, and the results showed an effective reduction of the acceleration levels induced in the isolation structures. For the purpose of prolonging the isolation system's life span of service, Tsai (2010) proposed a static dynamics interchangeable-ball pendulum system (SDI-BPS). Several general steel balls provided supports to long terms of service loadings. When an earthquake happened, these balls didn't work any more, and a damped steel ball surrounded by damping materials began to uphold the vertical loads and supply additional damping to the bearing by deforming the damping material. Kurita (2011) developed a similar device for seismic response reduction, and the peak acceleration amplitude was decreased by about 50-90%. Nanda (2012) considered that the base isolation in the form of pure friction (P-F), among all other isolation methods developed so far, was the simplest one, which could be easily applied to low cost brick masonry buildings. Furthermore, the P-F isolation

is one of the best alternatives for reducing earthquake energy transferred to superstructure during strong earthquake.

In all these studies, although the rolling friction isolation device reduces structural damage caused by earthquakes, the induced structural displacement may be very large and difficult to control (Kosntantinidis and Makris 2009, Lewis and Murray 1995). Therefore, some restoring devices, such as springs and dampers, are usually added to the isolation device to provide the restoring force, which can eliminate excessive relative displacement and reduce the structural residual displacement (Wei *et al.* 2014a, Wei *et al.* 2014b). In addition, the previous researches and applications usually assume all of the rolling friction coefficients on the contact surface as a constant value to simplify the calculation process of the structural seismic response. But the assumption is not reasonable in some sense (Wei *et al.* 2013, Wang *et al.* 2010, Yin and Wei 2013). Because the contact surface is usually rough in fact, and the according rolling friction coefficient on the contact surface is uneven (Begley and Virgin 1998, Flom and Bueche 1959). Theoretically, the uneven distribution of rolling friction coefficient may lead to great uncertainty in the structural seismic responses (Wei *et al.* 2015, Yim *et al.* 1980).

This paper artificially makes the uneven distribution of rolling friction coefficient to be concave as shown in Fig. 1. The rolling friction coefficient in the center of the contact surface is the smallest one, and it gradually increases when the relative displacement between the rolling ball and the ground increases. The friction coefficient increment of unit length is defined as the increment ratio  $R$  of the concave friction distribution. A spring and a damper are added to a contact surface with this concave friction distribution to form a spring-damper-rolling isolation system as shown in Fig. 1. The main purpose of this paper is to utilize a numerical analysis to detailedly analyze the impact of the concave friction distribution on the seismic performance of the spring-damper-rolling isolation system under different ground motions.

## 2. Spring-damper-rolling isolation system

Fig. 1 schematically describes an idealized spring-damper-rolling isolation system, namely a single degree-of-freedom structural system supported by a rolling isolation device, a damper, and an elastic spring element. In this system, the rolling device isolates the earthquake input motion and supports the superstructure. During a seismic event, it could induce friction force at the bottom of the structure to balance the inertial force developed in the superstructure, and importantly, it dissipates the seismic energy. The damper element has a similar function with that of the rolling device, namely producing a damping force and energy dissipation. The spring element remains elastic, and it is able to reduce the relative displacement between the structure and the ground and the residual displacement.

Despite the fact that the rolling device and the damper element can both dissipate the seismic energy, the forces induced by component are fundamentally different. The damping force produced by the damper is a function of the relative velocity, whereas the friction force provided by the rolling device is dependent on the structural mass, the rolling friction coefficient, and the relative motion or the tendency of relative motion (i.e., static friction force) between the structure and the ground.

The concave friction distribution could be achieved in practical applications. When a steel ball was rolling on a smooth surface made of steel, the rolling friction coefficient was about 0.005 which was very small. As the smooth surface got rougher along the path of motion in comparison

to that in the center of the contact surface, the rolling friction coefficient increased. A spring and a damper were easily added to a contact surface with this concave friction distribution to form a spring-damper-rolling isolation system as shown in Fig. 1.

### 3. Calculation process

This section defined the specific values for parameters of the spring-damper-rolling isolation system. Many calculation cases of the isolation system in Fig. 1 were obtained as a result of combing these parameters with different values.

#### 3.1 Structure model

As demonstrated in the related studies, the structure was built as a rigid body in the computer program since the stiffness of the isolation device was far less than that of the structure (Wei *et al.* 2014). The structure mass  $M$  was set to be 300t, the damping constants  $C$  adopted 100, 200, 300, 400 and 500 kN·s/m, and the spring constant  $K$  of the isolation device adopted 200, 400, 600, 800 and 1000kN/m, respectively. And thus all of the structural natural periods were 7.69, 5.44, 4.44, 3.84 and 3.44 s, respectively. Because they were much larger than the predominant period of the common earthquakes, the probability of resonance was quite little. Shear keys were considered and designed in the isolation device to meet the requirements under normal loadings and failure was only permitted under earthquakes.

For the concave friction distribution, the rolling friction coefficient in the center of the contact surface was the smallest one which was assumed to be a constant value of 0.005 in this paper. When the relative displacement between the structure and the ground increased, the rolling friction coefficient on the contact surface increased. The slope of the concave distribution of friction coefficient as shown in Fig. 1 was defined as the increment ratio  $R$  of the concave friction distribution. And  $R$  in Fig. 1 was assumed to be 0, 0.005, 0.010, 0.015, 0.020, 0.025 and 0.030  $m^{-1}$ , respectively.

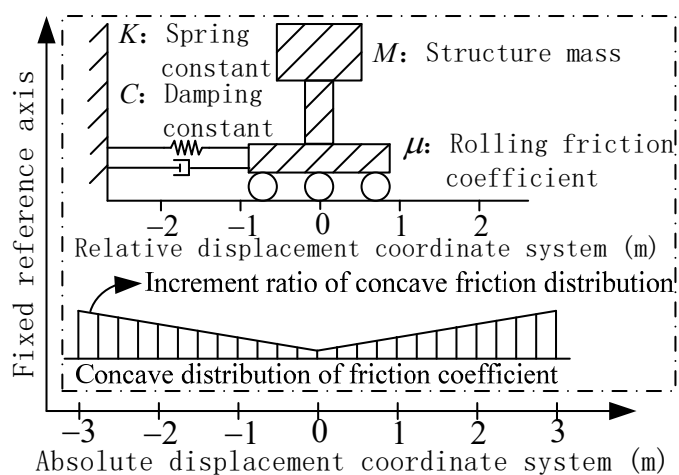
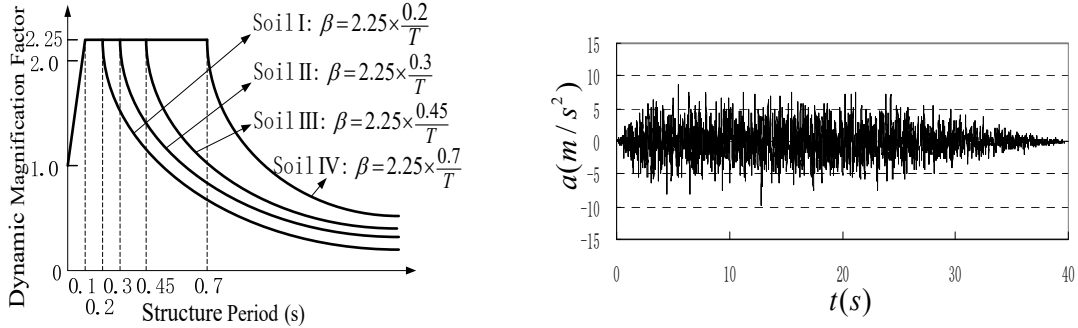


Fig. 1 A spring-damper-rolling isolation system



(a) Elastic response spectrum in Chinese criteria (JTJ 004-89)

(b) A representative accelerogram corresponding to the soil profile I

Fig. 2 Earthquake input

### 3.2 Ground motion

As for each response spectrum for the soil profile (SP) I, II, III, and IV, which were from stiff to soft, in Chinese criteria as shown in Fig. 2(a) (JTJ 004-89) (1989), one accelerogram was generated by Simqke procedure to be the ground motion input of the structural model (Fahjan and Ozdemir 2008). One representative ground motion out of four was shown in Fig. 2(b).

### 3.3 Calculation cases

175 cases were obtained by combining 1 structure mass, 5 damping constants, 5 spring constants and 7 increment ratios of the concave friction distribution.

As for each case, each accelerogram in section 3.2 was input as the ground motion, whose peak ground accelerations (PGA) were adjusted to be 0.2, 0.4, 0.6 and 0.8 g, respectively. And thus 2800 cases were generated for the further calculation.

Then each case was calculated by the computer program compiled by the authors (Wei *et al.* 2014). In order to mathematically describe the motion of the ground and the structure, the coordinate system of the absolute displacement is defined in Fig. 1. The terms  $a_e$ ,  $v_e$ ,  $d_e$  are defined as the absolute acceleration, absolute velocity, and absolute displacement of the ground, respectively. Similarly,  $a_s$ ,  $v_s$ ,  $d_s$  are the corresponding absolute response terms of the structure.

The relationship between  $v_e$  and  $v_s$  could yield three different scenarios as follows:

(1)  $v_e > v_s$ . This case indicates that a relative motion occurs between the structure and the ground surface, which belongs to the rolling state. Since the ground moves faster than the structure in the coordinate system of Fig. 1, the resultant force acting on the structure should be in combination of the spring force, the damping force, and the rolling friction force, which can be expressed as  $[\mu mg + K(d_e - d_s) + C(v_e - v_s)]$ .

(2)  $v_e < v_s$ . In this case, a relative motion occurs between the structure and the ground, and it belongs to the rolling state. However, the direction of the rolling friction force is opposite to that of the spring force and the damping force since the structure moves relatively faster than the ground. In this regard, the resultant force becomes  $[-\mu mg + K(d_e - d_s) + C(v_e - v_s)]$ .

(3)  $v_e = v_s$ . This implies no relative motion between the structure and the ground, and it is the non-rolling state. However, this state should be considered from two situations: i) static condition

of the structure and the ground prior to the start of ground shaking; and ii) the dynamic synchronization between the structure and the ground. The equation of motion can be expressed as  $ma_e = \pm F_{friction} + K(d_e - d_s) + C(v_e - v_s)$ , where  $F_{friction} \leq \mu mg$ . In these two situations, the equation is simplified as  $ma_e = \pm F_{friction} + K(d_e - d_s)$  since  $v_e = v_s$ , or  $|[a_e - K(d_e - d_s)/m]| = F_{friction}/m \leq \mu g$ . In order to estimate the response of the structure at next time step, it is necessary to compare the following two terms, namely  $|[a_e - K(d_e - d_s)/m]|$  and  $\mu g$ :

(1) when  $|[a_e - K(d_e - d_s)/m]| \leq \mu g$ , it means that the inertia force developed in the structure is not able to trigger the relative movement between the structure and the ground. Therefore, the acceleration  $a_s$  of the structure is equal to the ground acceleration  $a_e$ .

(2) when  $|[a_e - K(d_e - d_s)/m]| \geq \mu g$ , the instantaneous ground motion is intense enough to break the balance state and develop the relative movement between the structure and the ground. Therefore, the resultant force acting on the structure could be mathematically expressed as  $[\pm \mu mg + K(d_e - d_s) + C(v_e - v_s)]$ . Note that the sign of the rolling friction force depends on the direction of the ground acceleration  $a_e$ . In this case,  $v_e$  is different from  $v_s$ .

Prior to reach the next time step, if  $|[(v_s - v_e) + K(d_e - d_s)\Delta t_i/m + C(v_e - v_s)\Delta t_i/m]| \leq \mu g\Delta t_i$  and  $|[a_e - K(d_e - d_s)/m - C(v_e - v_s)/m]| \leq \mu g$ , the system will move to case (1), i.e.,  $v_e = v_s$ , where  $\Delta t_i = t_i - t_{i-1}$  and  $t_i$  is the  $i$ th time of the ground motion input. With knowledge of this, the relationship between the rolling state and the non-rolling state can be determined.

Based on the above calculation process, a large number of seismic responses were obtained. The following sections discussed those results, but only classical and common results were discussed in detailed manner due to space limitations while other results were considered but not listed.

#### 4. Structural peak acceleration

Figs. 3, 4, 5, 6 relatively show the effect of the increment ratio  $R$  of concave friction distribution, the damping constant  $C$ , the spring constant  $K$  and the site type of soil profile (SP) on the ratios of the structural peak acceleration to the ground peak acceleration (PGA).

Since the structure is assumed rigid in this study, its peak acceleration developed in the structure directly relates to the peak force developed at the base of the system, which is equal to sum of the spring force, damping force, and friction force based on force equilibrium. By definition, the spring force is the function of the displacement of the system relative to the ground. An increase of the rolling friction coefficient helps to dissipate the earthquake energy, and thereby decreases the relative displacement and further the spring force. However, for the system with a lower friction coefficient, spring force developed is larger than the friction force. As such, the total force in the system is subjected to a decrease at this stage as shown in Fig. 3, which is more significant when the spring constant is large. As the friction coefficient continues to increase, the friction force gradually becomes the dominant component that results in an increase of the resultant force and thereby the peak acceleration as shown in Fig. 3, which is more significant when the damping constant is large.

An increase in the damping constant helps to dissipate the earthquake energy and thereby decrease the relative displacement and further the spring force. However, for the system with low

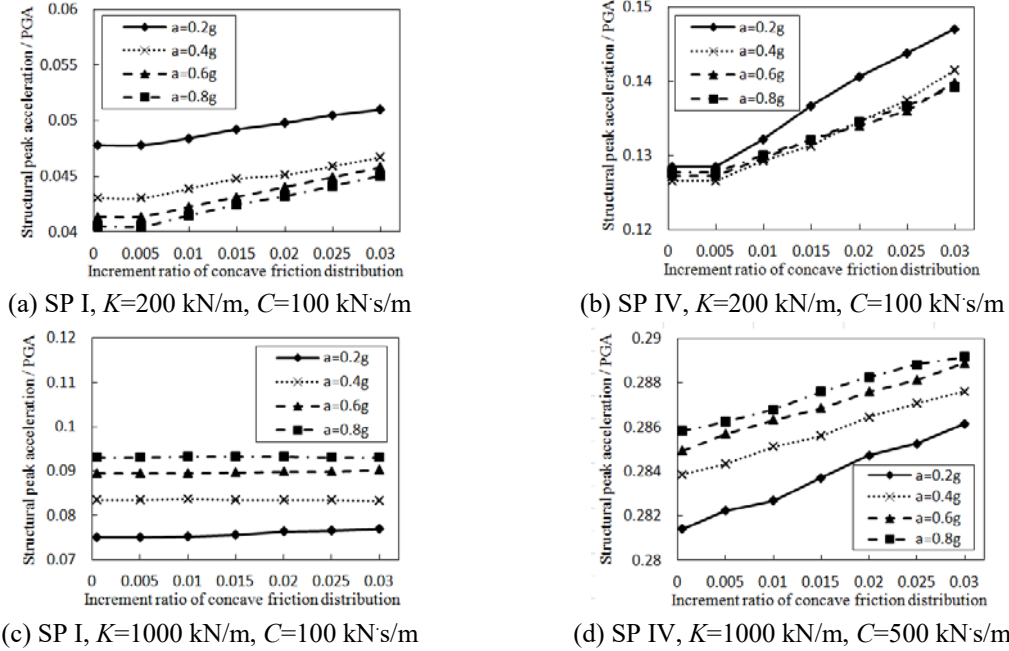


Fig. 3 Effect of the increment ratio  $R$  of concave friction distribution on the structural peak acceleration

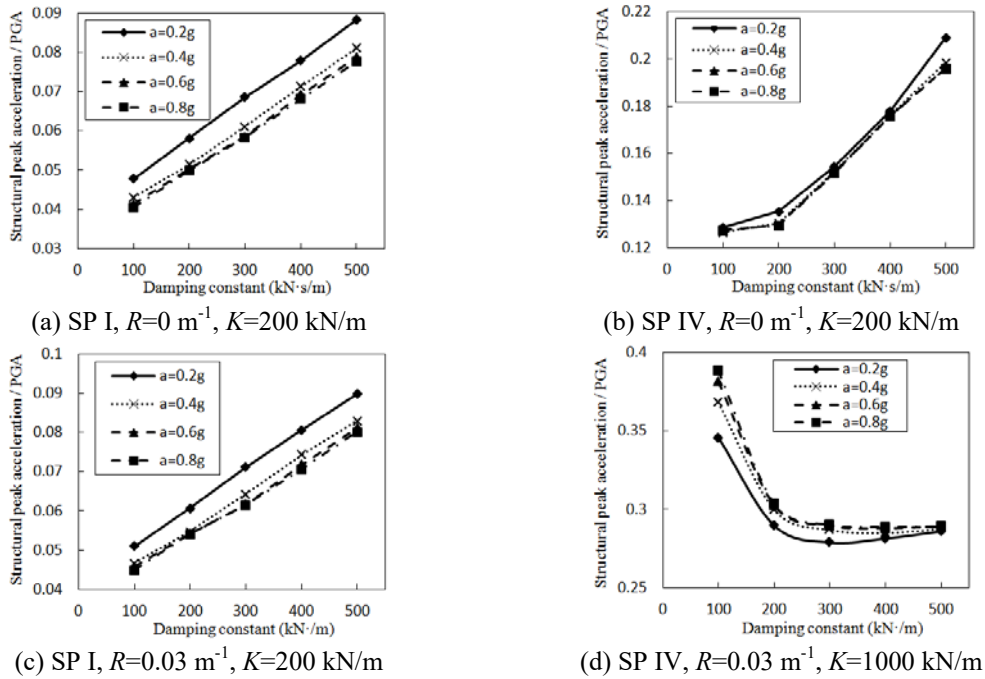


Fig. 4 Effect of the damping constant  $C$  on the structural peak acceleration

spring constant, damping force developed is larger than the spring force. As such, the total force in

the system is subjected to an increase at this stage as shown in Fig. 4. As the spring constant continues to increase, the spring force gradually becomes the dominant component resulting in a decrease of the resultant force and thereby the peak acceleration as shown in Fig. 4. However, when the damping constant continuously increases, the resultant force and the peak acceleration become to increase slowly.

When the spring constant is large, the analysis results also suggest that the peak acceleration do not monotonically vary with the rolling friction coefficient and the damping constant as shown in Figs. 3 and 4. Critical rolling friction coefficient and damping constant exist to achieve a minimized peak acceleration. When the system has a small damping constant, the critical rolling friction coefficient is usually large, and similar trend for the critical damping constant.

In contrast, as the spring can't dissipate any seismic energy, increasing the spring constant of the spring-damper-rolling isolation system in Fig. 1 subjected to an earthquake naturally increases the spring force. In this case, the structural relative displacement is reduced and the friction force of the isolation device subsequently decreases due to the concave friction distribution of the contact surface in Fig. 1. In addition, an increase of the spring constant has negligible impact on the fluctuation of the damping force. In general, the increment of the spring force is larger than the reduction of the friction force, and accordingly, their combination force and the structural peak acceleration increase as shown in Fig. 5. However, sometimes the increment of the spring force may be less than the reduction of the friction force, and it results in the decreasing of the combination force and the structural peak acceleration as shown in Fig. 5. This case mainly occurs when the spring constant and the site type of soil profile are large. Under these conditions, the isolation layer is not easy to roll, and the isolation system nearly has natural period components. Simultaneously, a softer site type of soil profile means more long-period components of the

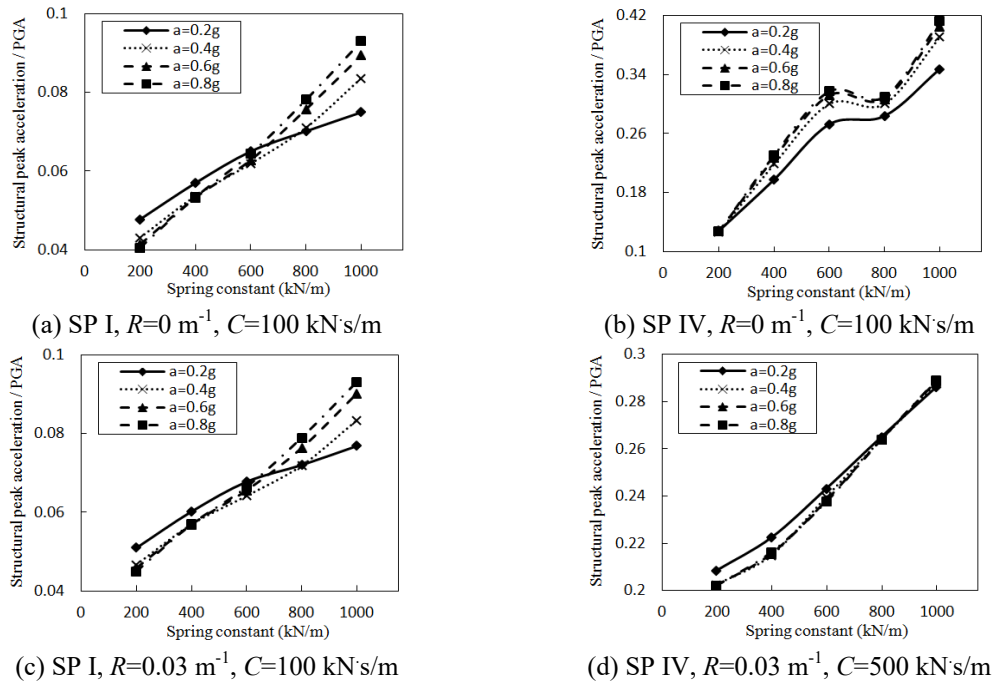


Fig. 5 Effect of the spring constant  $K$  on the structural peak acceleration

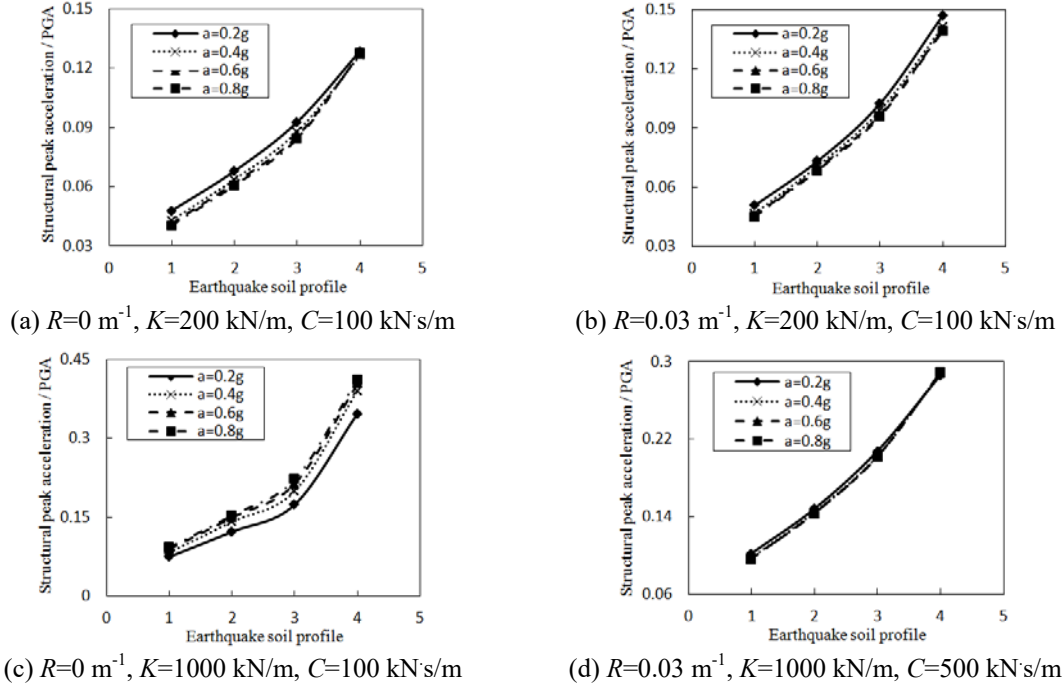


Fig. 6 Effect of the site type of soil profile (SP) on the structural peak acceleration

corresponding seismic wave. In theory, the local resonance phenomenon is easier to appear under these conditions, and leads to the sudden increment of the structural relative displacement and the according sudden increment of the combination force of the spring force and the friction force. However, if the spring constant continuously increases, the natural period of the isolation structure is changed and shifts away from the local resonance region, which results in the sudden reduction of the structural relative displacement and the relevant sudden reduction of the combination force of the spring force and the friction force. These sudden increment and reduction phenomena eventually form the fluctuations of the structural peak acceleration as shown in Fig. 5. Overall, in aspect of only reducing the structural acceleration, the best choice is to reduce the spring constant. It is also noted that, for a system with zero spring constant and zero damping constant, the peak acceleration developed should not exceed  $\mu g$  from theoretical calculation.

For the same isolation system in Fig. 1, a larger earthquake, including a softer site type of soil profile and a larger PGA, or a larger spring constant means that the spring performs a more important role in the isolation system, which would function more like a traditional elastic isolation system. In this case, more damping provided by increasing the increment ratio of concave friction distribution and damping constant will result in a more significant decrease of the structural peak acceleration as shown in Fig. 5.

The earthquake is a highly unpredictable natural disaster. The inaccurate estimations of earthquake, which is normal at present, affect the structural acceleration response. When the site type of soil profile is softer or PGA is larger, both the spring force and the friction force increase due to the concave friction distribution of the contact surface as shown in Fig. 1. Finally, the combination force and the structural peak acceleration increase as shown in Fig. 6.

## 5. Structural peak relative displacement

Figs. 7, 8, 9, 10 relatively show the effect of the increment ratio of concave friction distribution, the damping constant, the spring constant and the site type of soil profile on the ratios of the structural peak relative displacement to the ground peak displacement (PGD).

The ordinate axis in the Figs. 7 through 10, adopting the form of 'Structural peak. relative displacement/PGD', is based on two considerations. On the one hand, it is convenient to draw all of the calculation results under different earthquakes in the same graph. On the other hand, it is preferable to demonstrate the effects of the rolling friction coefficient which will be detailedly illustrated in the following paragraph.

Theoretically, the rolling friction not only dissipates the earthquake energy to reduce the structural relative displacement, but also shortens the structural natural period. The latter function can be clearly seen from the graphs. In theory, as the elastic structure has a fixed natural period, altering PGA of the same seismic wave will not change the ratios of the structural peak relative displacement to the peak absolute displacement of the ground motion. However, in the graphs, these ratios are obviously changed by altering PGA. It can be seen from these graphs that the friction action has a great impact on the structural natural period, and the impact is limited by the magnitude of the earthquake. In an event of a weak earthquake, the rolling state of the isolation system in Fig. 1 is not obvious and the rolling friction has a significant limitation on the structural vibration. In this case, the structural natural period dramatically and sensitively changes. When the earthquake is too weak to overcome the rolling friction to trigger the relative displacement of the isolation device in Fig. 1, the natural period of the isolation structure will be equal to that of the non-isolation structure.

In addition, based on Figs. 7 through 10, it is concluded that the concave friction distribution is conducive to reducing the structural relative displacement. This can be detailedly explained in the following paragraph.

When  $v_e > v_s$  at some time during an earthquake, the friction force  $\mu mg$  provides a forward acceleration component  $\mu g$ , referring to the coordinate system in Fig. 1, to the isolated structure. In this case, there are two possible cases due to the influence of the concave friction distribution:

(1) If the moving structure is on the left of its original position at this moment, it means that the rolling friction coefficient on the contact surface is increasing, and the according increment of the structural acceleration  $\mu g$  is conducive to reducing the structural relative displacement.

(2) In contrast, if the moving structure is on the right of its original position now, the rolling friction coefficient on the contact surface is decreasing which is opposite to case (1). And accordingly, the reduction of the structural acceleration  $\mu g$ , however, is also conducive to reducing the structural relative displacement.

There are similar rules in the case of  $v_e < v_s$ .

In summary, the concave friction distribution exactly has a function of reducing the structural relative displacement. And in theory, a larger increment ratio of concave friction distribution implies a smaller structural peak relative displacement as shown in Fig. 7. Specific effects are divided into two cases:

(1) When the increment ratio of concave friction distribution in Fig. 1 increases from a little value, the corresponding friction action is so insignificant that a slight ground motion may result in the vibration of the structure, which is more like a traditional elastic isolation system. In this case, increasing the rolling friction coefficient, due to increasing the increment ratio of concave friction distribution, can efficiently dissipate the earthquake energy and reduce the structural relative

displacement. In addition, the increment of the rolling friction coefficient resulting from increasing the increment ratio of concave friction distribution shortens the structural natural period so that it can also decrease the structural relative displacement. Finally, it can be concluded that the interaction of above two effects of increasing the increment ratio of concave friction distribution from a little value efficiently decreases the structural relative displacement.

(2) In contrast, if the increment ratio of concave friction distribution in Fig. 1 continuously increases on the basis of a large value which is larger than that of case (1), the vibration of the structure is so difficult that the energy dissipation capacity of the rolling friction becomes insignificant. In this case, as the increment ratio of concave friction distribution increases, the structural relative displacement continuously decreases, however, with very low speed. In addition, with the continuously enlarged increment ratio of concave friction distribution, the structural natural period gets shorter and is closer to some long-period wave components of an earthquake. And accordingly, the decreasing trend of the structural relative displacement gradually diminishes and is even transformed into the increasing trend. Based on the two aspects above, increasing the increment ratio of concave friction distribution, on the basis of a large value, finally results in slowly decreasing the structural relative displacement.

When a larger spring constant is adopted in the isolation structure in Fig.1 or a larger spring force is resulted from a severe earthquake, the spring performs a more important role in the

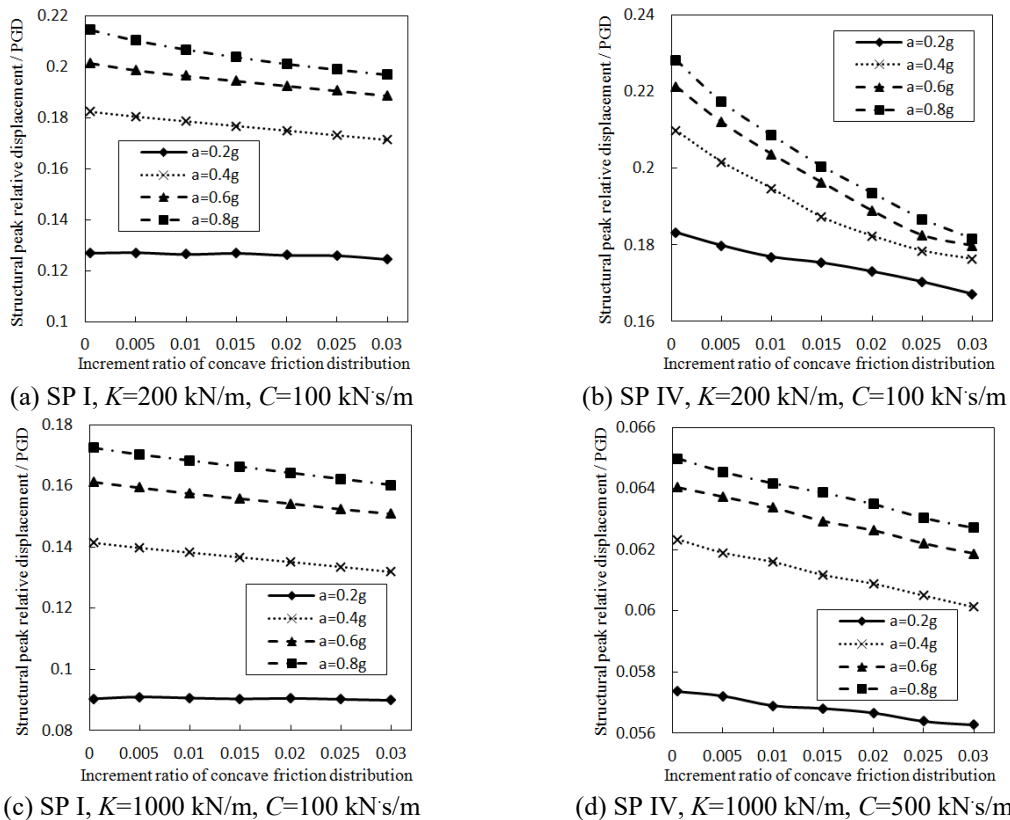


Fig. 7 Effect of the increment ratio  $R$  of concave friction distribution on the structural peak relative displacement

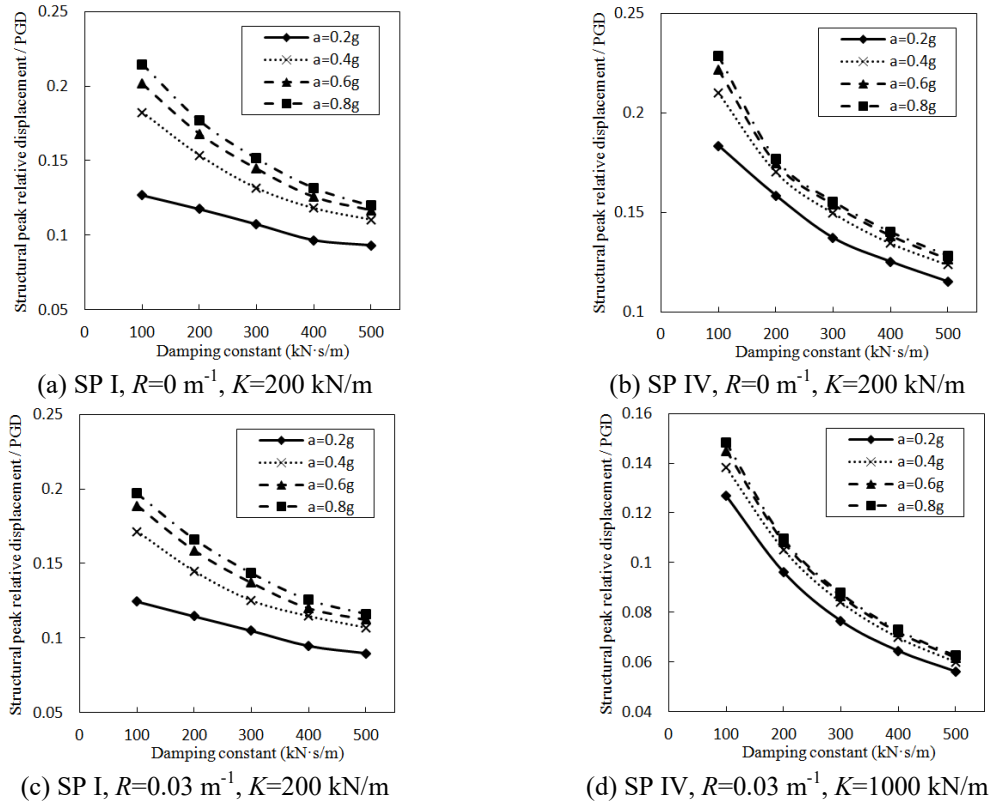


Fig. 8 Effect of the damping constant  $C$  on the structural peak relative displacement

vibration of the isolation system, which is more like a traditional elastic isolation system. In this case, increasing the increment ratio of concave friction distribution significantly reduces the structural relative displacement as shown in Fig. 7. Only when the increment ratio of concave friction distribution increases to a much larger value, is the energy dissipation capacity of the rolling friction significantly reduced. And accordingly, the structural relative displacement begins to decrease slowly.

An increase in the damping constant is also able to dissipate the earthquake energy and thereby decrease the relative displacement as shown in Fig. 8. A critical damping constant shows that the energy dissipation is different as the damping constant varies. When the damping constant is extremely small, low intensity shaking could make the structure to vibrate significantly. As the relative displacement is large, the energy dissipated by the damping force becomes large. Therefore, an increase of damping constant will considerably decrease the relative displacement. When the damping constant is increased to a certain value, the relative displacement is dramatically decreased which results in a decrease of the energy dissipation by the damper. A further increase of damping constant only results in steady state response of relative displacement.

Although the effects of the rolling friction and the damping constant on the relative displacement are quite similar, the way how each affect the relative response is different. The major difference is that the rolling friction is able to change the natural periods and the displacement ratios of the system, which depend on the earthquake intensity. However, this

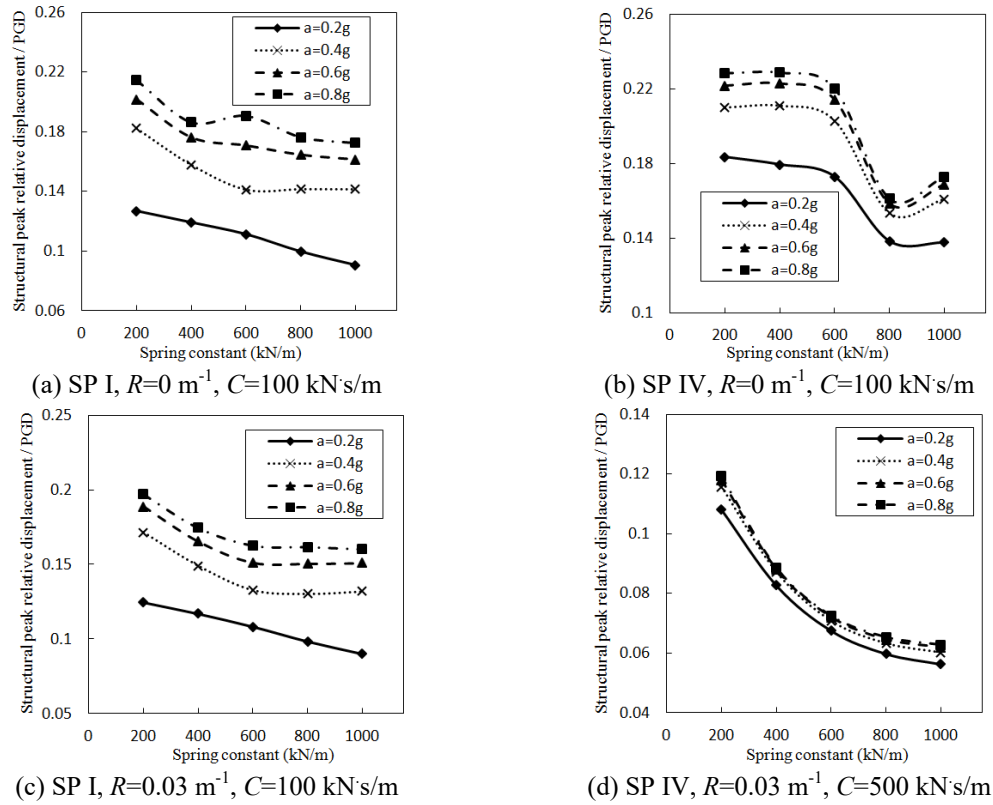


Fig. 9 Effect of the spring constant  $K$  on the structural peak relative displacement

phenomenon becomes less pronounced with an increase of the damping constant. In addition, critical rolling friction coefficient and damping constant occur where the peak relative displacement are greatly reduced. When the system has a small damping constant, the critical rolling friction coefficient is usually large, and similar trend for the critical damping constant.

In addition, increasing the spring constant shortens the structural natural period so that the structural relative displacement decreases as shown in Fig. 9. Simultaneously, as analyzed in the above paragraph, a larger spring constant or a severer earthquake leads the isolation system to vibrate more like a traditional elastic isolation system. This mechanism is validated by the phenomenon that all the corresponding ratios of the structural peak relative displacement to the peak absolute displacement of the ground motion related to different PGA are closer to each other when comparing to that of other cases. In this case, if the structural natural period approaches some long-period wave components of an earthquake, the structural peak relative displacement may fluctuate up and down as shown in Fig. 9, which implies that resonance happens. The fluctuation will be significantly reduced with an increase of the damping constant rather than the rolling friction coefficient.

Most of ground motion characteristics of earthquake can't be accurately predicted at present, and the inaccurate estimations of earthquake inevitably affect the structural displacement responses as shown in Fig. 10. When other parameters of the isolation system in Fig. 1 are unchanged, the softening of soil profile extends the wave periods of an earthquake and accordingly

increases the absolute displacement of the ground motion. If the spring constant, the damping constant and the increment ratio of concave friction distribution of the isolation system in Fig.1 are all small and PGA is little, the induced structural absolute acceleration, velocity and displacement under earthquakes are inevitably small. As the structural relative displacement is defined as the difference between the structural absolute displacement and the ground absolute displacement, it increases as a result of the opposite trends of the above two absolute displacements induced by softening the soil profile of an earthquake and simultaneously setting the above parameters with small values of the isolation systems. Fortunately, because the concave friction distribution and the damper are conducive to decreasing the structural relative displacement, it weakens the increasing trend of the structural relative displacement. In contrast, when the spring constant is set to be a large value or the rolling friction coefficient increases due to the concave friction distribution and the increased PGA, the according isolation system has a relatively short natural period and is prone to resonance under the condition of softening soil profile to extend the wave periods of an earthquake. The resonance leads to the appearance of the peak value of the structural peak relative displacement. However, as the rolling friction and the damper can dissipate the earthquake energy and the concave friction distribution can change the structural natural period, the peak value of the structural peak relative displacement resulting from resonance isn't very large.

The inaccurate estimations of PGA also significantly affect the structural displacement responses, but in a different way as shown in Fig. 10. By keeping other parameters of the isolation

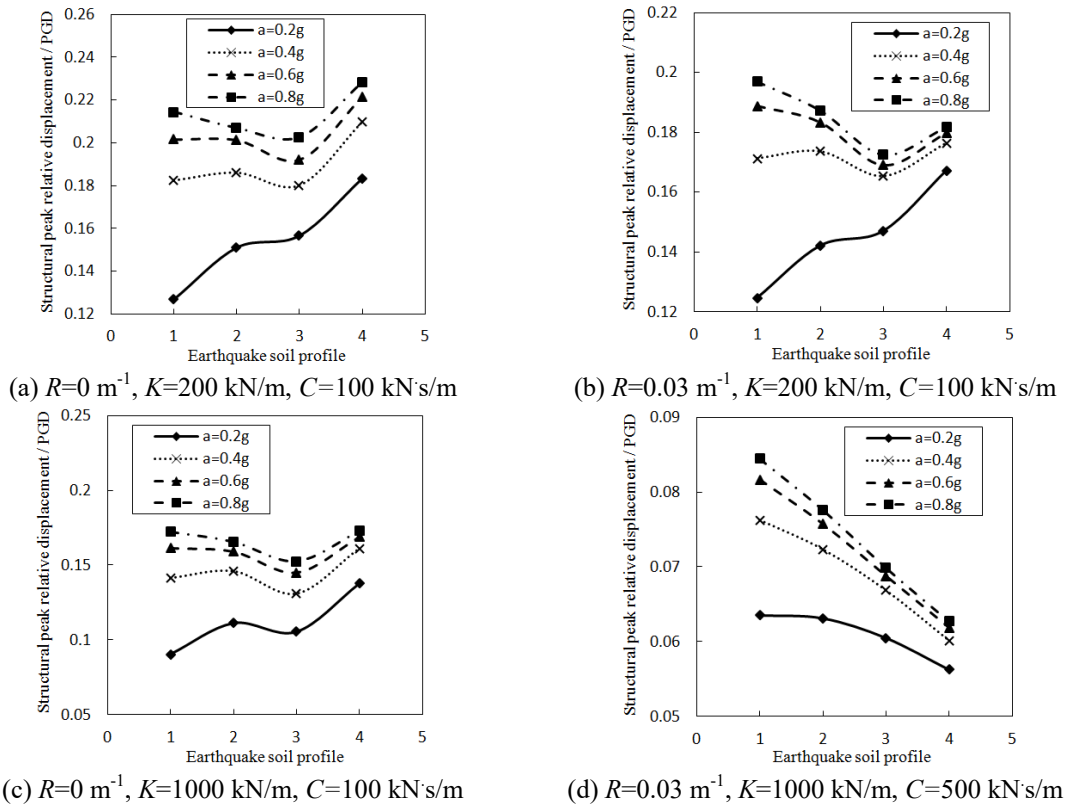


Fig. 10 Effect of the site type of soil profile (SP) on the structural peak relative displacement

system in Fig. 1 the same, only increasing PGA increases the absolute displacement of the ground motion more efficiently than the absolute displacement of the structure. And accordingly, the structural relative displacement, i.e., the difference between the structural absolute displacement and the ground absolute displacement, increases.

## 6. Structural residual displacement

To reduce the repair cost of the isolation structure, the isolator is expected to roll back to the original position without a significant residual displacement after earthquakes. Therefore, this section analyzes the residual displacement of the isolation system in Fig. 1 subjected to different ground motions.

Theoretically, the structural residual displacement is influenced by the spring, the damper, the rolling friction and the earthquake. The spring of the isolation system in Fig. 1 tends to restore the structure to the original position, while the rolling friction prefers to accommodate the structure to any place, and prevents the structure from rolling back to the original position. The damper is different with the rolling friction, and it doesn't prevent the restoration of the structure. Based on the statics equilibrium between the spring force  $K\Delta$  and the friction force  $\mu mg$ , the structural theoretical residual displacement  $\Delta$  in Fig. 1 can be obtained from the equation  $K\Delta = \mu mg$ . As the rolling friction coefficient  $\mu$  is the function of the residual displacement  $\Delta$  due to the concave friction distribution, it is expressed as  $\mu = 0.005 + R\Delta$ , in which 0.005 is the smallest rolling friction coefficient in the center of the contact surface as described in section 3.1 and  $R$  is the increment ratio of the concave friction distribution. And thus the equation  $K\Delta = \mu mg$  is further expressed as  $K\Delta = (0.005 + R\Delta)mg$ . Finally, the structural theoretical residual displacement is  $\Delta = 0.005mg/(K - Rmg)$  or  $\Delta = 0.005/(K/mg - R)$ . It infers from this equation that the spring is beneficial to decreasing the structural residual displacement, while the rolling friction, including the rolling friction coefficient in the center of the contact surface and the concave friction distribution, is against decreasing the structural residual displacement.

However, the conclusion above is only based on the statics mechanics. The feeble ground motion before the earthquake completely stops will break the equilibrium state above and induce the structure to a new equilibrium condition in which the residual displacement will be less than the theoretical value of  $\Delta = 0.005/(K/mg - R)$ .

It is concluded from the above discussions that the structural residual displacement is less than the value of  $\Delta = 0.005/(K/mg - R)$  in spite of any conditions. Before the structure completely stops, the isolator will vibrate on the contact surface between  $\pm 0.005/(K/mg - R)$  for a moment, and the influence factors on the relative displacement as analyzed in section 5 will also affect the structural residual displacement which is the relative displacement just when the structure stops moving.

At the moment, the concave friction distribution is conducive to restoring the structure to the original position, and accordingly decreases the structural residual displacement, especially when an isolation system in Fig. 1 with a larger spring constant is subjected to an earthquake with the larger PGA in the softer soil profile.

As for the spring-damper-rolling system, though increasing the damping constant decreases the structural residual displacement, the influence depends on the value of the spring constant. When the spring constant is very small, the theoretical residual displacement range between  $\pm 0.005/(K/mg - R)$  is relatively large. In this case, increasing the damping constant effectively reduces

the structural residual displacement. Nonetheless, as the damping constant increases to a certain value, the impact of the damping constant on the structural residual displacement will be feebler due to the fact that the damper with large damping constant will prevent the structure from moving fast and freely. In contrast, when the spring constant is very large, the theoretical residual displacement range between  $\pm 0.005/(K/mg - R)$  is relatively small. In this condition, as the damping constant increases, the decreasing trend of the structural residual displacement is relatively faint.

Because the earthquake has no function of restoring the structure to the original position, the changing of the soil profile or PGA of the earthquake only leads to the random and disorganized results of structural residual displacement. The structural residual displacement not only seems to depend on the soil profile and PGA of the earthquake, but also is very sensitive to the detailed shape of earthquake wave. Even the minor changes of the terminal part of earthquake wave results in considerably different residual displacement.

Because the numerical analysis and the theoretical analysis above have completely consistent results, and the structural residual displacement of most calculation cases doesn't have any obvious variation law on the comprehensive impact of varied factors, these corresponding figures with irregular data are not presented herein due to space limitations.

## **7. Conclusions**

This paper investigates the seismic response of a spring-damper-rolling isolation system, and particularly analyzes the influence of rolling friction coefficients with concave distribution, damping constants, spring constants and other factors on the isolation performance. The main conclusions are drawn as follows:

- A small spring constant could yield a small peak acceleration of the system. However, an increase of the spring constant is able to dramatically decrease the relative peak and residual displacement of the structure. As for the damping constant, an increase could effectively decrease the relative displacement and residual displacement of the structure. However, its influence on acceleration response is not definite as it is affected by other system's properties including the spring constant, rolling friction coefficient, and input motion characteristics. When the concave distribution of rolling friction coefficient is concerned, an increase could effectively decrease the relative displacement of the structure. However, its influence on acceleration response is not definite as it is affected by other system's properties including the spring constant, the damping constant, and the input motion characteristics.

- As to achieve an optimal performance, a small spring constant could be designed to get a small peak acceleration. Based on the function that the residual displacement is always less than the theoretical value of  $\Delta = 0.005/(K/mg - R)$ , the appropriate increment ratio  $R$  of the concave friction distribution can be calculated to obtain the allowable residual displacement. And then, the appropriate damping constant can be obtained to significantly decrease the structural relative displacement and insignificantly increase the structural acceleration by calculation and statistics based on a series of design waves of ground motion.

- The analysis results also suggest that the peak acceleration and peak relative displacement do not monotonically vary with the rolling friction coefficient and the damping constant. Critical rolling friction coefficient and damping constant exist to achieve a minimized peak acceleration. Similarly, the critical values occur where the peak relative displacement are greatly reduced. When

the system has a small damping constant, the critical rolling friction coefficient is usually large, and similar trend for the critical damping constant. Therefore, in the optimization design of the general spring-damper isolation system or other similar systems influenced by the rolling friction or the slipping friction, the impact of friction must be considered in detail according to the actual situations. Otherwise, some optimized results will not be the optimum values.

- Both the damping force and the rolling friction force are able to dissipate earthquake energy, however, they differ in that the rolling friction component contributes the overall stiffness of the system and thereby potentially modifies the natural period of the system while the damping force insignificantly changes the system's natural period. Moreover, the lateral stiffness contributed by the rolling coefficient depends on the relative movement between the structure and the ground. For the case with small relative movement, the rolling friction component will greatly contribute and increase the lateral stiffness resulting in a stiff system with a low natural period. When the earthquake intensity is not high enough to trigger the relative movement, the natural period is equal to that of the fixed-base condition. In this regard, it is desirable to thoroughly evaluate the development of the rolling friction component of the spring-damper-rolling isolation systems prior to conduct its seismic design. Otherwise, there may be some errors in the calculation results of structural seismic response.

## Acknowledgements

This research is jointly supported by the National Natural Science Foundation of China under grant No. 51308549, 51378504 and 51478475, the Natural Science Foundations of Hunan Province under grant No.2015JJ3159, and the Innovation-driven Plan in Central South University under grant No. 2015CX006. The above financial support is greatly appreciated.

## References

- Antonyuk, E.Y. and Plakhtienko, N.P. (2004), "Dynamic modes of one seismic-damping mechanism with frictional bonds", *Int. Appl. Mech.*, **40**(6), 702-708.
- Begley, C.J. and Virgin, L.N. (1998), "Impact response and the influence of friction", *J. Sound Vib.*, **211**(5), 801-818.
- Chung, L.L., Kao, P.S., Yang, C.Y., Wu, L.Y. and Chen, H.M. (2015), "Optimal frictional coefficient of structural isolation system", *J. Vib. Control*, **21**(3), 525-538.
- Cui, S. (2012), "Integrated design methodology for isolated floor systems in single-degree-of-freedom structural fuse systems", Ph.D. Dissertation, State University of New York, Buffalo.
- Fahjan, Y. and Ozdemir, Z. (2008), "Scaling of earthquake accelerograms for non-linear dynamic analysis to match the earthquake design spectra", *The 14th World Conference on Earthquake Engineering, Chinese Society for Earthquake Engineering*, Beijing, China.
- Flom, D.G. and Bueche, A.M. (1959), "Theory of rolling friction for spheres", *J. Appl. Phys.*, **30**(11), 1725-1730.
- Guerreiro, L., Azevedo, J. and Muhr, A.H. (2007), "Seismic tests and numerical modeling of a rolling-ball isolation system", *J. Earthq. Eng.*, **11**(1), 49-66.
- Harvey, P.S. and Gavin, H.P. (2013), "The nonholonomic and chaotic nature of a rolling isolation system", *J. Sound Vib.*, **332**(14), 3535-3551.
- Harvey, P.S. and Gavin, H.P. (2014), "Double rolling isolation systems: a mathematical model and experimental validation", *Int. J. Non-Linear Mech.*, **61**(1), 80-92.

- Harvey, P.S. and Gavin, H.P. (2015), "Assessment of a rolling isolation system using reduced order structural models", *Eng. Struct.*, **99**, 708-725.
- Harvey, P.S., Wiebe, R. and Gavin, H.P. (2013) "On the chaotic response of a nonlinear rolling isolation system", *Physica D: Nonlinear Phenomena*, **256-257**, 36-42.
- Harvey, P.S., Zehil, G.P. and Gavin, H.P. (2014), "Experimental validation of a simplified model for rolling isolation systems", *Earthq. Eng. Struct. Dyn.*, **43**(7), 1067-1088.
- Ismail, M. (2015), "An isolation system for limited seismic gaps in near-fault zones", *Earthq. Eng. Struct. Dyn.*, **44**(7), 1115-1137.
- Ismail, M. and Casas, J.R. (2014), "Novel isolation device for protection of cable-stayed bridges against near-fault earthquakes", *J. Bridge Eng.*, **19**(8), 50-65.
- Ismail, M., Rodellar, J. and Pozo, F. (2014), "An isolation device for near-fault ground motions", *Struct. Control Hlth. Monit.*, **21**(3), 249-268.
- Ismail, M., Rodellar, J. and Pozo, F. (2015), "Passive and hybrid mitigation of potential near-fault inner pounding of a self-braking seismic isolator", *Soil Dyn. Earthq. Eng.*, **69**(2), 233-250.
- Jangid, R.S. (2000), "Stochastic seismic response of structures isolated by rolling rods", *Eng. Struct.*, **22**(8), 937-946.
- Jangid, R.S. and Londhe, Y.B. (1998), "Effectiveness of elliptical rolling rods for base isolation", *J. Struct. Eng.*, **124**(4), 469-472.
- JTJ004-89, Standard of the Ministry of Communications of P.R. China (1989), *Specifications of Earthquake Resistant Design for Highway Engineering*, China Communications Press, Beijing, China. (in Chinese)
- Kosntantinidis, D. and Makris, N. (2009), "Experimental and analytical studies on the response of freestanding laboratory equipment to earthquake shaking", *Earthq. Eng. Struct. Dyn.*, **38**(6), 827-848.
- Kurita, K., Aoki, S., Nakanishi, Y., Tominaga, K. and Kanazawa, M. (2011), "Fundamental characteristics of reduction system for seismic response using friction force", *J. Civ. Eng. Architec.*, **5**(11), 1042-1047.
- Lee, G.C., Ou, Y.C., Niu, T.C., Song, J.W. and Liang, Z. (2010), "Characterization of a roller seismic isolation bearing with supplemental energy dissipation for highway bridges", *J. Struct. Eng.*, **136**(5), 502-510.
- Lewis, A.D. and Murray, R.M. (1995), "Variational principles for constrained systems: Theory and experiment", *Int. J. Non-Linear Mech.*, **30**(6), 793-815.
- Nanda, R.P., Agarwal, P. and Shrikhande, M. (2012), "Base isolation system suitable for masonry buildings", *Asian J. Civ. Eng. (Building and Housing)*, **13**(2), 195-202.
- Ortiz, N.A., Magluta, C. and Roitman, N. (2015), "Numerical and experimental studies of a building with roller seismic isolation bearings", *Struct. Eng. Mech.*, **54**(3), 475-489.
- Ou, Y.C., Song, J.W. and Lee, G.C. (2010), "A parametric study of seismic behavior of roller seismic isolation bearings for highway bridges", *Earthq. Eng. Struct. Dyn.*, **39**(5), 541-559.
- Siringoringo, D.M. and Fujino, Y. (2015), "Seismic response analyses of an asymmetric base-isolated building during the 2011 Great East Japan (Tohoku) Earthquake", *Struct. Control Hlth. Monit.*, **22**(1), 71-90.
- Tsai, C.S., Lin, Y.C., Chen, W.S. and Su, H.C. (2010), "Tri-directional shaking table tests of vibration sensitive equipment with static dynamics interchangeable-ball pendulum system", *Earthq. Eng. Eng. Vib.*, **9**(1), 103-112.
- Wang, S.J., Hwang, J.S., Chang, K.C., Shiao, C.Y., Lin, W.C., Tsai, M.S., Hong, J.X. and Yang, Y.H. (2014), "Sloped multi-roller isolation devices for seismic protection of equipment and facilities", *Earthq. Eng. Struct. Dyn.*, **43**(10), 1443-1461.
- Wang, Y.J., Wei, Q.C., Shi, J. and Long, X.Y. (2010), "Resonance characteristics of two-span continuous beam under moving high speed trains", *Latin Am. J. Solid. Struct.*, **7**(2), 185-199.
- Wei, B., Cui, R.B. and Dai, G.L. (2013), "Seismic performance of a rolling-damper isolation system", *J. Vibroeng.*, **15**(3), 1504-1512.
- Wei, B., Dai, G.L., Wen, Y. and Xia, Y. (2014), "Seismic performance of an isolation system of rolling friction with spring", *J. Central South Univ.*, **21**(4), 1518-1525.
- Wei, B., Xia, Y. and Liu, W.A. (2014), "Lateral vibration analysis of continuous bridges utilizing equal

- displacement rule”, *Latin Am. J. Solid. Struct.*, **11**(1), 75-91.
- Wei, B., Yang, T.H. and Jiang, L.Z. (2015), “Influence of friction variability on isolation performance of a rolling-damper isolation system”, *J. Vibroeng.*, **17**(2), 792-801.
- Yim, C.S., Chopra, A.K. and Penzien, J. (1980), “Rocking response of rigid blocks to earthquakes”, *Earthq. Eng. Struct. Dyn.*, **8**(6), 565-587.
- Yin, C.F. and Wei, B. (2013), “Numerical simulation of a bridge-subgrade transition zone due to moving vehicle in Shuohuang heavy haul railway”, *J. Vibroeng.*, **15**(2), 1062-1068.

CC